Hydrodynamic Design of Contra-Rotating Propeller for the Ships

Hassan Ghassemi[1], Roya Shademani[2]

Abstract: This paper describes a contra-rotating propeller (CRP) system to calculate the hydrodynamic characteristics and then design the optimum operational condition to be installed on two different large bulk carriers and VLCC. The method is based on boundary element method (BEM) to obtain the hydrodynamic performance of any complicated configuration such as CRP system, and then the optimum propeller data is obtained by the systematic method at the design condition. The researchers prepared a software package code, namely SPD, which has model mesh generation, solver and numerical output results. The comparison of the propulsive performance was made between the propeller alone and CRP arrangement. Major finding include optimal agreement between predictions using the numerical code and experimental data for both ships.

Keywords: CRP, Boundary Element Method, Optimum Efficiency

طراحی هیدرودینامیکی پروانه سری با چرخش معکوس برای کشتی‌ها

حسن قاسمی، رویا شادمانی

چکیده: مقاله حاضر، طراحی و محاسبات هیدرودینامیکی سیستم پیش برنده پروانه سری با چرخش معکوس (CRP) را برای دو نوع شناور ارائه می دهد. روش عددی جهت تحلیل عملکرد هیدرودینامیکی پروانه ها بر پایه جریان پتانسیل با استفاده از روش المان مرزی مورد استفاده قرار گرفته است. ضرایب هیدرودینامیکی پروانه ها برای دو شناور VLCC و فله بر بزرگ در دو حالت تک پروانه ای و CRP مورد مقایسه و تحلیل قرار می گیرد. محاسبات شامل نیروهای تراست، گشتاور و راندمان پروانه ها می باشد که با نتایج تجربی مقایسه شده است. نتایج قابل قبولی از این روش عددی برای پروانه های تکی و پروانه های سری در مقایسه با مقادیر تجربی بدست آمده است.

واژه‌های کلیدی: پروانه سری، روش المان مرزی، راندمان بهینه

---

1. Associate Professor, Department of Marine Technology, Amirkabir University of Technology, Tehran, Iran (gsemi@cic.aut.ac.ir)

2. M. S. Student, Department of Marine Technology, Amirkabir University of Technology, Tehran, Iran (roya.shademani@gmail.com)

1. Introduction

The main aims of the marine propulsor designers are to increase thrust, diminish torque, improve efficiency and to save energy. Most conventional propulsors are working behind the ship hull where the flow is non-uniform, unsteady and also limitation of the propeller diameter due to ship stern exists. Another case is that the single propeller generates torque and so there are some designing for rudder or design the asymmetric stern hull to overcome this torque. To solve all disadvantageous problems, CRP solve all of them means canceling the torque, improving the performance [1, 2].

The history of CRP goes back to when a patent was applied by Ericsson (the inventor in 1836) to 45 feet ship. In 1909 and 1939, Italian Navy and US Navy had experimented CRP on a 46 feet and 70 feet steam ship, respectively. Rutundi [3] made a comparative test between CRP and conventional propeller for a 3500 tons naval training ship and has reported an 18% improvement in the propulsive performance.

Since then, CRP has well been used for torpedoes, small vessels, and of course for aircraft, but there is a difficulty in producing a reliable CR shafting which can support the large power for application to large merchant ships. In 1988, MHI (Japan) has succeeded in retrofitting 4200 GT with a CRP [4], and in the same year, IHI (Japan) has completed the shop test of Juno's CRP system at the outset. Having been equipped with this CRP system, Juno dealt with the official trial in witch she has achieved a 15% power saving. After that, some other experimental researches have been done at NMRC (in Japan) (before the name was SRI) by Ukon, [5, 6, 11, 13].

From the numerical approach during two decades, some work has been done to obtain a better understanding of the system in order to predict its effect on hydrodynamic performance. Yang C-J [1] and Islam et al. [8] used lifting surface theory and vortex lattice method to calculate the blade loading.

Recently, more attention is being drawn to the development of the contra-rotating podded propulsor (CRPP) system for ship propulsion because of its attractively high energy saving rate as well as lower cavitation and better hydrodynamic performance.

In the current arrangement, a CRPP is placed at the forward end of a pod which is aligned with the local inflow. The powering and cavitation experiments show the performance prediction agree well with the measurement.

Nishiyama and Sakamoto [10] designed a CRP system at IHI and on bulk carrier and VLCC.
This paper deals with the following areas:
- Numerical method of BEM
- Mesh generation
- Design concept of CRP behind of the ship
- Design concept of CRPP
- Application of the CRP system on the ship
- Systematic design

In this paper, a contra-rotating podded propulsor design with a tractor pod for large ships is tackled by numerical method. The calculated results are predicted well with experimental measurements. Systematic design is finally employed to the two ships types (Bulk carrier and VLCC) to obtain the designed points.

2. Design concept of CRP
2.1. Procedure of CRP designing

With the principal particularities of the hull and the main engine given, a CRP can be designed for any single propeller, namely, through reiteration of the following two steps:
(1) Propeller design in uniform flow: try to find for an optimum design that fulfills the given engine power and revolution speed; then
(2) Modification by considering the non-uniform flow: the propeller designed thus is further modified, so as to better adapt to the non-uniform flow over what has already been considered macroscopically in step (1), in such terms as propeller cavitation, propeller-induced vibration, and strength of blade for the propeller performance in non-uniform flows.

2.1. Designing CRP in uniform flow

There are two approaches in the design of CRP: one based on lifting surface theory [9], and other utilizing the design diagram based on open water tests on systematic CRP model series [5]. More precise results could be expected from the systematic series data than from the theoretical approach. However, a review of the past reports for CRP, the method based on series test data can be found.

Fig. 1 depicts the design procedure and algorithm. Here, the relation between ship speed and resistance (R_T-V_s) for the hull, self propulsion test or some empirical formulae (t, w, η_R), the number of blade (Z) and axial distance between two propellers (x_A) are given. According to systematical method and flow chart, first estimate the revolution number of propeller and its diameter. Then using numerical code (SPD=Ship Propeller Design), the hydrodynamic characteristics (open water) of propeller alone and CRP system are calculated.

How to calculate the optimum efficiency from the open water diagram? This is the systematic method to obtain the optimum design of the propeller for the ship. From the resistance and self propulsion test or some empirical formulae, the following relations may be expressed:

For single conventional propeller:

$$K_T = \frac{T}{\rho n^2 D^4} = \frac{T}{\rho D^2 V_A^2} . J^2 \tag{1}$$

$$= \frac{R_T}{(1-t)\rho D^2 \left(V_S (1-\overline{w})\right)^2} . J^2 = A.J^2$$

For CRP system:

$$K_T = \frac{T_F + T_A}{\rho n_F^2 D_F^4} \tag{2}$$

$$= \frac{R_T}{(1-t)\rho D_F^2 \left(V_S (1-\overline{w})\right)^2} . J^2 = B.J^2$$

This K_T is quadratic function of J and intersects with open water curves of $K_T - J$ and the optimum solution is obtained from the intersection point, so all the coefficients are obtained from this point (K_T, K_Q, η_o, J). Then, the thrust and torque are obtained from the following:

$$T = K_T(J_{n,D})\rho n^2 D^4, \qquad T_{\text{Calculated}(i+1)} \geq T_{\text{Required}(i)} \qquad (3)$$

$$Q = K_Q(J_{n,D})\rho n^2 D^5, \qquad Q_{i+1} \leq Q_i$$

$$K_Q = \frac{n_F Q_F + n_A Q_A}{\rho n_F{}^2 D_F{}^5} \qquad (4)$$

$$J = \frac{V_A}{n_F D_F} \quad \eta_O, = \frac{J}{2\pi}\frac{K_T}{K_Q} \qquad (5)$$

The reiteration is continued unless the thrust should be bigger than the required one and torque should be less than the previous stage.

3. Numerical approach
3.1. Potential based boundary element method

Suppose the forward propeller of a CRP with Z_F blades rotates in the left hand (counter-clockwise) direction at a constant evolution number η_F, while the aft propeller Z_A blades in the right hand (counter-clockwise) direction at η_A, and the CRP as a whole advances at a constant speed V_A.

Assuming inviscid, incompressible and irrotational flow in the volume around and inside the body, a potential function exists for the perturbation velocity ϕ created by the propeller movement in the volume which satisfies the Laplace's equation. By applying Green's theorem for perturbation velocity potential ϕ at any field point on the body surface, we can get the following integral equation on the propeller and its trailing vortex wake.

$$2\pi\phi(P) = \int_{S_B}\left\{\phi(q)\frac{\partial}{\partial n_q}\left(\frac{1}{R(p;q)}\right) - \frac{\partial\phi(q)}{\partial n_q}\left(\frac{1}{R(p;q)}\right)\right\}dS \qquad (6)$$

$$+ \int_{S_W}\Delta\phi(q)\frac{\partial}{\partial n_q}\left(\frac{1}{R(p;q)}\right)dS$$

$R(p;q)$ is the distance from the field point p to the singularity point q. This equation may be regarded as a representation of the velocity potential in terms of a normal dipole distribution of strength $\phi(P)$ on the body surface S_B, a source distribution of strength $\partial\phi/\partial n$ on S_B, and a normal dipole distribution of strength $\Delta\phi(q)$ on the trailing wake surface S_W.

3.2. Boundary conditions

The strength of the source distribution in equation (6) is known from kinematic boundary condition (KBC) as follows:

$$\frac{\partial\phi}{\partial n} = -\vec{V}_I \cdot \vec{n} = -\left[V_A + \vec{\omega}\times\vec{r}\right]\vec{n} \qquad (7)$$

where $\vec{n}$ denotes the outward normal unit vector.

The strength of dipole distribution is unknown and equal to the perturbation potential on the propeller or to the potential jump in the trailing vortex wake. On the wake surface S_w, the velocity is considered to be continuous while the potential has a jump across the wake. It is expressed in the perturbation potential as:

$$\Delta\left(\frac{\partial\phi}{\partial n}\right)_{S_W} = \left(\frac{\partial\phi}{\partial n}\right)^B - \left(\frac{\partial\phi}{\partial n}\right)^F = 0 \qquad (8)$$

$$(\Delta\phi)_{S_W} = \phi^B - \phi^F = \Gamma \qquad (9)$$

where indexes B and F mean back and front sides of the propeller, respectively.

Another important physical boundary condition is the Kutta condition and its implementation. This equal pressure Kutta condition is applied to determine the unknown $\Delta\phi_{TE}$ of the dipole strength on the wake surface. In the numerical calculation, the pressure Kutta condition at the back and front surfaces of the trailing edge (TE), can be expressed as:

$$\Delta p_{TE} = p_{TE}{}^B - p_{TE}{}^F = 0 \qquad (10)$$

A direct solution of the resulting system of equations obtained from discretized Green's formula for the perturbation velocity potential (6), along with equation (10) is difficult due to the nonlinear character of the equation (6) therefore, an iterative solutions algorithm is employed to solve the problem. We focus on the numerical implementation in the following section.

Discretization of equation (6) leads to a linear system of algebraic equations for the unknown ϕ as:

$$2\pi\phi_i = \sum_{N_P=1}^{2}\left(\sum_{k=1}^{K}\sum_{j=1}^{N_{tot}}D^k{}_{ij}(\phi_j)\right) + \sum_{N_P=1}^{2}\left(\sum_{k=1}^{K}\sum_{j=1}^{M}\sum_{l=1}^{N_W}W^k{}_{ijl}(\Delta\phi_j)\right) \qquad (11)$$

$$+ \sum_{N_P=1}^{2}\left(\sum_{k=1}^{K}\sum_{j=1}^{N_{tot}}S^k{}_{ij}\left(\frac{\partial\phi}{\partial n}\right)_j\right), \quad i = 1,2,...,N_{tot}, \; where N_{tot}$$

$$= K \times N \times M$$

Where $D^k{}_{ij}$, $W^k{}_{ijl}$ (dipole distributions on body and wake surfaces) and $S^k{}_{ij}$ (source distribution on body) are influence coefficients on panel j acting on the control point of panel i. Those influence coefficients are nearly evaluated analytically. The use of quadrilateral surface panels instead of planar panels has been found to be important for the convergence of the present potential based boundary element method. It is found to be especially so when applied to the highly skewed propeller and twisted shape.

3.3. Calculation of induced velocity

From Green's theorem in the potential field, equation (6), we can alternatively construct in the velocity field.

Taking the gradient of the perturbation velocity potential at any field point, the induced velocity which can be expressed as:

$$4\pi\vec{v}(p) = \int_{S_B} \left\{ \phi(q)\nabla_p \frac{\partial}{\partial n_q}\left(\frac{1}{R(p;q)}\right) - \frac{\partial\phi(q)}{\partial n_q}\nabla_p\left(\frac{1}{R(p;q)}\right) \right\} dS \qquad (12)$$

$$+ \int_{S_W} \Delta\phi\phi\nabla_p \frac{\partial}{\partial n_q}\left(\frac{1}{R(p;q)}\right) dS$$

Here, from the discretization of the body and wake, and assuming the potential ϕ and the value of $\frac{\partial\phi}{\partial n}$ are constant within each panel. Then, equation (12) can be written as:

$$4\pi\vec{v}_i = \sum_{N_P=1}^{2}\left(\sum_{k=1}^{K}\sum_{j=1}^{N_{tot}}(\phi_j)\nabla_p C^k_{ij}\right) + \qquad (13)$$

$$\sum_{N_P=1}^{2}\left(\sum_{k=1}^{K}\sum_{j=1}^{M}(\Delta\phi_j)\nabla_p W^k_{ijl}\right)$$

$$+ \sum_{N_P=1}^{2}\left(\sum_{k=1}^{K}\sum_{j=1}^{N_{tot}}\left(\frac{\partial\phi}{\partial n}\right)_j^k \nabla_p S^k_{ij}\right), \quad i = 1,2,...,N_{tot}$$

Where $\nabla_p C^k_{ij}$, $\nabla_p W^k_{ijl}$ and $\nabla_p S^k_{ij}$ are the velocity influence coefficients. Those velocity coefficients can be evaluated analytically by assuming that the surface elements are approximated by a number of quadrilateral hyperboloidal panels.

Calculations of the velocity influence were more sensitive than the potential coefficient, and also the required storage was three times more than the storage of the potential coefficient. There was one big advantage that the velocities can directly be obtained for any field points.

The induced velocity diagram of the CRP is shown in Fig. 2, where u_a and u_t denotes the axial and circumferential induced velocities, respectively. Since the interaction between two propellers, the total induced velocities may be expressed as follows:

$$(u_a)_i = (u_a)_{ii} + (u_a)_{ij} \qquad (14)$$

$$(u_t)_i = (u_t)_{ii} + (u_t)_{ij}$$

For two fore and aft propellers, it is given:

$$(u_a)_1 = (u_a)_{11}, \qquad (u_a)_2 = (u_a)_{22} + (u_a)_{21} \qquad (15)$$

$$(u_t)_1 = (u_t)_{11}, \qquad (u_t)_2 = (u_t)_{22} + (u_t)_{21}$$

Where $(u_{a(t)})_{ij}$ implies the axial or circumferential velocities at *i-th* propeller induced by the *j-th* propeller. The subscript 1 and 2 denote the forward or aft propeller, respectively. We observe that $(u_a)_{21}$ is zero and $(u_t)_{21}$ is very small and may be neglected.

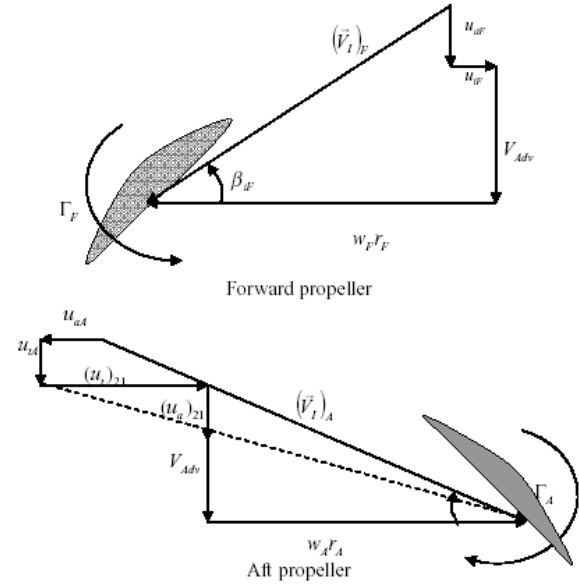The hydrodynamic pitch angle and resultant velocities to the fore and aft propellers are expressed as follows:

Fig. 1. Relative velocities at blade section of CRP

$$\tan\beta_{iF} = \frac{V_{Adv} + u_{aF}}{\omega_F r_F + u_{tF}} \qquad (16)$$

$$\tan\beta_{iA} = \frac{V_{dvA} + u_{aA} + (u_a)_{21}}{\omega_F r_F - u_{tA} + (u_t)_{21}}$$

Inflow velocity to the fore propeller may be obtained by:

$$\vec{V}_{IF} = \vec{V}_{Adv} + \vec{u}_{aF} + \vec{\omega}_F \times \vec{r}_F - \vec{u}_{tF} \qquad (17)$$

$$V_{IF} = \sqrt{(V_{Adv} + u_{aF})^2 + (2\pi r_F n_F - u_{tF})^2}$$

Inflow velocity to the aft propeller is expressed by:

$$\vec{V}_{IA} = \vec{V}_{Adv} + \vec{u}_{aA} + (\vec{u}_a)_{21} + \vec{\omega}_A \times \vec{r}_{AF} - \vec{u}_{tA} + (\vec{u}_t)_{21} \qquad (18)$$

$$V_{IA} = \sqrt{(V_{Adv} + u_{aA} + (u_a)_{21})^2 + (2\pi r_A n_A - u_{tA} + (u_t)_{21})^2}$$

4. Numerical results and discussion

4.1. Application of the CRP system on the bulk carrier and VLCC

The researchers applied the method on two CRP for two different ship types where the model tests have been done in IHI and were available [9] and [10]. Main dimensions for bulk carrier and VLCC are given in Table 1. For each vessel, conventional propeller and CRP have been used and the results are compared. The CRP5022 and conventional propeller (single propeller MP588) for the bulk carrier and CRP5029 and MP620 for VLCC have been selected. The principal particularities of both CRP propeller and single propeller are given in Tables 2 and 3.

4.2. Grid generation

As known that the BEM is dealing with boundary of the body, so the grid generation is the necessary starting point for numerical implementation. The coordinate of the discretized surface should be sufficiently accurate since any inaccuracy can lead the hydrodynamic pressure

to become noisy. According to our experience, the hyperboloidal quadrilateral element seems to be better than other elements like triangular and super element. Higher order element (quadratic or cubic order) is very complicated way to apply although it gives more precise results. This is our future plan to be done. However, for the present calculation and prepared SPD code, the hyperboloidal quadrilateral elements are used to discretize the whole body (hub and two propellers).

4.3. Hydrodynamics characteristics and determination of design point

Numerical results of the open water characteristics are compared with the experimental data for the CRP and conventional propellers. It is shown that the numerical results of the present method are very accurate and in optimal agreement with the experimental data for the open-water characteristics.
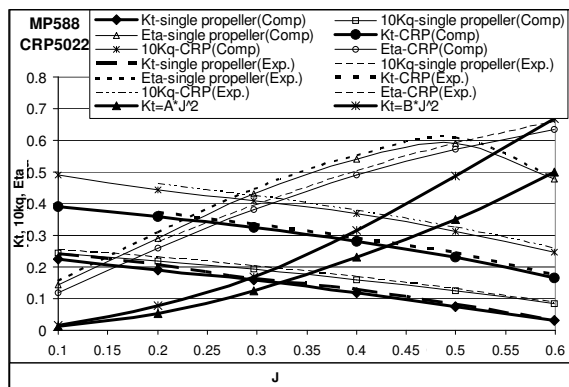
Fig. 2. Comparison of open water characteristics of conventional and CRP propellers for the Bulk-Carrier and the determination of design point

Using the equations (1) and (2), $(K_T = A.J^2, K_T = B.J^2)$, in Figs. 2 and 3, intersection points are obtained between the thrust coefficients for each conventional and CRP propellers.
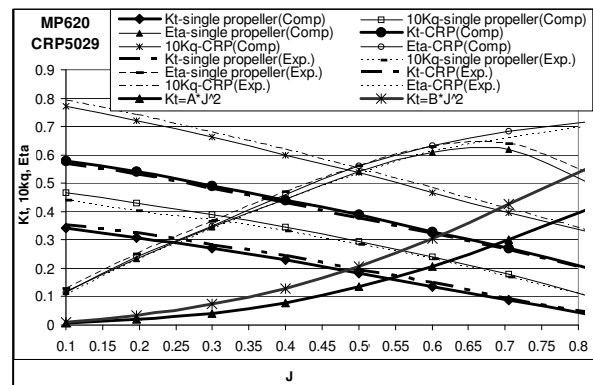
Fig. 3. Comparison of open water characteristics of conventional and CRP propellers for the VLCC and the determination of designed point

Table 1. Main dimensions of the bulk carrier and VLCC

Ship Parameter	Bulk Carrier (Juno)	VLCC
Length (LBP)[m]	178.0	314.0
Breadth [m]	28.4	58.0
Depth [m]	10.72	19.5
Dead Weight	37000	–
Speed at full load [Knot]	15	16

Table 2. Principal particulars of CRP and single propellers for bulk carrier

Propeller / Type Parameters	Single Propeller MP588	Contra-Rotating propeller CRP5022	
		Forward	Aft
D [mm] for model tset	277.6	250.0	213.9
D [m] for ship	5.23	4.71	4.03
Boss ratio	0.20	0.20	0.18
Z	4	4	5
P/D	0.6	0.70	0.80
EAR	0.62	0.42	0.45
Skew angle [deg.]	7	20	20
Direction of rotation	Left hand	Left hand	Right hand
Section	MAU	MAU	MAU

Table 3. Principal particulars of CRP and single propellers for VLCC

Propeller / Type **Parameters**	**Single Propeller MP620**	**Contra-Rotating propeller CRP5029**	
		Forward	**Aft**
D [mm] (model)	269.3	250.0	221.0
D [m] (VLCC)	10.20	9.47	8.37
Boss ratio	0.15	0.20	0.18
Z	5	4	5
P/D	0.79	0.92	0.93
EAR	0.55	0.35	0.35
Skew angle [Deg.]	20	20	18
Direction of rotation	Left hand	Left hand	Right hand
Section	MAU	MAU	MAU

5. Conclusions

In this paper, the researchers numerically calculated the open water characteristics of the conventional and CRP and obtained the optimum operational condition for the large vessel using BEM. According to the results, the following conclusions are drawn:

- The present method can be applied to any complicated propeller configuration and determine the open water characteristics.
- The CRP system may raise the propeller efficiency around 2-3 percent at design condition for the present system.
- Designed point is determined based on the highest efficiency which is matched with the generated propeller and ship required thrusts.

References

[1] Yang, C-J, Tamashima, M., Wang, G., Tamazaki R. and Kuizuka, H., "Prediction of the steady performance of Contra-rotating Propeller by Lifting Surface Theory", Transaction of the West-Japan Society of Naval Architects, Vol. 83, 1992.

[2] Nakamura, S., Ohta, T., Yonekura, K., Sasajima, T. and Saki, K., "World's First Contra-rotating Propeller System Successful Fitted to a Merchant Ship, The Motor Ship", Proceedings of 11th International Marine Propulsion Conf. 9-10 March 1989.

[3] Rutundi, C. F., "Trials of the Training Ship Cristoforo Colombo with two Screws on a Common Axis", Trans. Institution of Naval Architects, 1934.

[4] Lee, C-S, Kim, Y. G., Baek, M-C., Yoo, J-H., "Numerical Prediction of Steady and Steardy Performance of Contra-rotating Propellers", Journal of Hydrospace Technology, Vol. 1 No. 1, 1995, 29-40.

[5] Chen, B. Y-H, Tseng, C. L., "A Contra-rotating Propellers Design for a High Speed Patrol Boat with Pod Propulsion", FAST' 95.

[6] Ukon, Y., Ohashi, K., Fujisawa, J., Hasegawa, J., "Propulsive Performance of a Contra-rotating Podded Propulsor", T-Pod Conference, Newcastle, April 2004.

[7] Chenjun, Y., Guiqiang, W., "Hydrodynamic Performance of Contra-rotating Propellers (CRP) Numerical Analysis, China Society of Naval Architecture and Marine Engineering", Vol. 7, 1992.

[8] Islam, M. F., Veitch, B., Bose N., Liu P., "Numerical Study of Hub Taper Angle Podded propeller Performance, J. of Marine Technology", Vol. 43, No. 1, January 2006, 1-10.

[9] Nishiyama, S., Sakamoto, Y., Fujino, R., "Contra-rotating Propeller System for Large Merchant Ships", Technical Bulletin of IHI, 1991.

[10] Nishiyama, S., Sakamoto, Y., Ishida, S, Fujino, R. and Oshima, M., "Development of Contra-rotating Propeller for Juno – A 37,000 DWT Class Bulk Carrier", Trans. SNAME , Vol. 98, 1990.

[11] Bjarrne, E., "Systematic Studies of contra-rotating Propellers for Merchant Ship", Proc. IMAS'73, 1973, 49-59.

[12] Ghassemi, H., Allievi, A., "A Computational Method for the Analysis of Fluid Flow and Hydrodynamic Performance of Conventional and Podded Propulsion Systems", Journal of Oceanic Engineering International, Vol. 3, No. 2, 1999.

[13] Ukon, Y. et. al. "On the Design of Contra-rotating Propellers – Application to High Speed Container Ship", Trans. Of the West –Japan Society of Naval Architects, Vol. 25, 1988, 52-64.